Electromagnetics

Magnetic Localization for an Electromagnetic-Based Haptic Interface

Alaa Adel[1], Mohanad Mansour[1], Mina M. Micheal[1], Ahmed Abdelmawla[1], Islam S. M. Khalil[2], and Sarthak Misra[2,3]

[1] Department of Mechatronics Engineering, German University in Cairo, New Cairo 11432, Egypt
[2] Department of Biomechanical Engineering, University of Twente, 7522 NB Enschede, The Netherlands
[3] Department of Biomedical Engineering and University Medical Centre Groningen, University of Groningen, 9713 AV Groningen, The Netherlands

Received 4 Feb 2019, revised 3 Mar 2019, accepted 22 Mar 2019, published 28 Mar 2019, current version 23 Apr 2019.

Abstract—In this letter, we develop a magnetic localization system for an electromagnetic-based haptic interface (EHI). Haptic interaction is achieved using a controlled magnetic force applied via an EHI on a magnetic dipole attached to a wearable finger splint. The position of the magnetic dipole is estimated using two identical arrays of three-dimensional magnetic field sensors in order to eliminate the magnetic field generated by the EHI. The measurements of these arrays are used to estimate the position of the magnetic dipole by an artificial neural network. This network maps the field readings to the position of the magnetic dipole. The proposed system is experimentally validated under four cases of the magnetic field generated by the EHI. These cases are likely to be encountered during the haptic rendering of virtual shapes. In the absence of the magnetic field, the mean absolute position error (MAE) is 0.80 ± 0.30 mm ($n = 125$). Static and sinusoidal magnetic fields are applied, and the MAEs are 1.26 ± 0.43 mm ($n = 125$) and 0.91 ± 0.33 mm ($n = 125$), respectively. A random time-varying magnetic field is applied, and the MAE is 0.86 ± 0.33 mm ($n = 125$). Our statistical analysis shows that the repeatability of the magnetic localization is acceptable regardless of the field generated by the EHI, at $\alpha = 0.05$ and 95% confidence level.

Index Terms—Electromagnetics, haptic rendering, localization, magnetic instruments, position estimation.

I. INTRODUCTION

In recent years, electromagnetic-based haptic interfaces (**EHI**s) have obtained considerable attention due to their effectiveness in medical simulation applications [Hu 2005]. The EHIs are classified into two groups: Lorentz-forces interfaces [Berkelman 1996, 2000, Salcudean 1997] and untethered interfaces [Berkelman 2012, 2013, Brink 2014, Seif 2017]; the latter is achieved using two methods: first, a stylus-based type where the haptic sensation is achieved via a magnetic force exerted on the dipole of an interaction stylus [Tong 2018] and second, a wearable-based type where the magnetic dipole is attached to a wearable device [Zhang 2016]. The second type produces static magnetic forces regardless of the position of the operator. The implication of using this technique is that it requires a relatively large number of coils to render all features of complex objects [Adel 2017]. This problem has been solved by the incorporation of a position-sensing device into the haptic system [Adel 2018], and an impedance-type haptic rendering algorithm has been implemented using an optical localization device. However, this type of devices has limitations, such as occlusion and sensitivity to illumination [Moeslund 2006, Kim 2012]. These limitations can be eliminated by using a magnetic-based localization system to estimate the position of the magnetic dipole based on its field data [Weitschies 1994, Schlageter 2001, Hu 2005, 2010]. The applications of this system include localization of endoscopic capsules [Di Natali 2013, Yim 2013, Popek 2017] and the development of motion capture systems for human–computer interaction [Hashi 2006, Ma 2011].

It is desirable to isolate the field of the magnetic dipole from the variable field generated by the EHI for the integration between EHI and magnetic localization system. For instance, a 5 degrees-of-freedom localization system for a magnetic capsule has been developed by Son [2016]. This capsule is actuated by an external source of a magnetic field using an omnidirectional electromagnet. The field produced by the actuator is modeled and subtracted from the measured data to obtain the field of the capsule. A magnetic position sensing and force feedback generated by a single electromagnetic coil for a magnetic stylus using an array of 16×16 Hall effect sensors have been developed by Berkelman [2018]. They have observed that the field generated by the coil interferes with the field generated by the stylus, and results in position estimation error. This problem has been solved directly by disregarding sensor measurements below a given threshold. However, this solution is not suitable for a planar configuration of electromagnetic coils supplied by a time-varying current input. In addition, modeling error of the field generated by a magnetic source is inversely proportional to the distance from this source to the point of measurement [Griffiths 1999, Petruska 2013]. Therefore, the modeling error decreases as the distance between the magnetic sensors and coils increases, and as a consequence, sensors with relatively high resolution are required and the compactness of the EHI is decreased.

In order to overcome the mentioned problems, we develop a magnetic localization system that does not depend on the precalculated magnetic field map of the EHI. The localization system consists of two arrays of three-dimensional (**3-D**) magnetic field sensors. These

Corresponding author: Islam S. M. Khalil (e-mail: i.s.m.khalil@utwente.nl).
A. Adel and M. Mansour are co-first authors.
Digital Object Identifier 10.1109/LMAG.2019.2908149

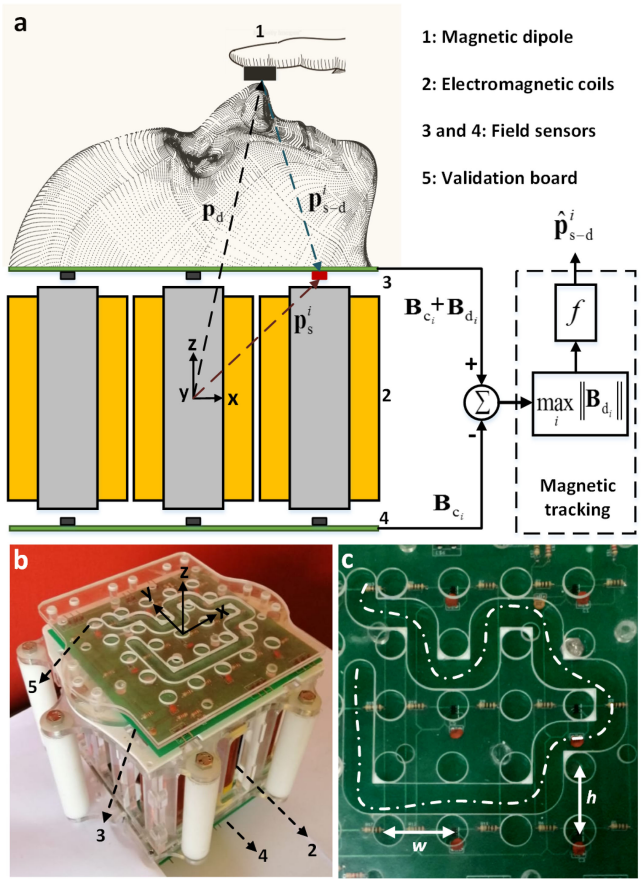

Fig. 1. Localization system is developed for an EHI. (a) Schematic representation shows a magnetic dipole (1) at a position $\mathbf{p}_d$ and a planar configuration of electromagnetic coils (2). The magnetic localization system consists of two identical arrays of 3-D magnetic field sensors. The first (3) and second (4) arrays are fixed above and below the EHI, respectively. (b) EHI is integrated to the two sensor arrays. (c) Validation board (5) is located above the upper array of the magnetic field sensors ($w = 21.5$ mm and $h = 21.5$ mm) at height of 9 mm.

arrays are mounted above and below the EHI, as shown in Fig. 1(a). The subtraction of the magnetic field between these two arrays provides the field of the magnetic dipole. The accuracy and repeatability of the localization system are validated under four different cases of the magnetic field generated by the EHI, i.e., zero (Case 1), static (Case 2), sinusoidal (Case 3), and time-varying magnetic field (Case 4). The remainder of this letter is organized as follows. Section II provides design and development of the magnetic-based localization system. Section III presents the experimental results of the position estimation under the mentioned cases. Finally, Section IV concludes this letter.

II. DEVELOPMENT OF A MAGNETIC LOCALIZATION SYSTEM

The EHI provides a controlled magnetic force on a magnetic dipole attached to a wearable finger splint. A magnetic localization system is used to estimate the position of the dipole using two arrays of magnetic field sensors [see Fig. 1(a)].

A. System Description

The EHI consists of a planar array of electromagnetic coils, a magnetic dipole, and a magnetic localization system [see Fig. 1(b)]. The array comprises nine coils; each has inner and outer diameter of 24 and 38 mm, respectively. The height of the coil and the length of its carbon steel core are 100 and 110 mm, respectively. Each of the electromagnets is independently supplied with current using electric drivers (MD10C, Cytron Technologies Sdn Bhd, Kuala Lumpur, Malaysia). These coils exert a magnetic force on a cylindrical neodymium magnet (S-10-10-N, N45, nickel-plated, Supermagnete, Gottmadingen, Germany) with length and diameter of 10 mm and an axial magnetization of 1.07×10^6 A $\cdot$ m^{-1}. The position of the dipole is estimated by a magnetic localization system. This system consists of two identical arrays of magnetic field sensors, each array ($n = 9$) contains 3-D Hall effect sensors (3-D magnetic sensor TLV493DA1B6, Infineon Technologies AG, Munich, Germany). The sensitivity of the sensors is 0.1 mT within a range of $\pm$130 mT, and they are validated using a calibrated three-axis digital teslameter (Senis AG, 3MH3A-0.1%-200 mT, Neuhofstrasse, Switzerland). The Hall effect sensor can detect the magnetic dipole in a workspace of 50 mm $\times$ 50 mm $\times$ 50 mm. The two arrays are located at the same height of 14 mm from the EHI. This sensor is located at the center of the corresponding coil. The sensor reading is provided using I^{2}C interface with 12-bit data resolution for each measurement direction. A MyRIO control board (MyRIO-1900, National Instruments, Austin, TX, USA) is used for the data acquisition from these sensors and to control the coils. The total time to acquire all the sensors readings and to estimate the position is 13 ms. A validation board is fabricated for the experimental validation of the localization system, as shown in Fig. 1(c). This board is located above the upper array of the magnetic field sensors with a height of 9 mm. It has 25 holes with a diameter of 10 mm and a slot. These holes are fabricated to fix the magnetic dipole, and the slot guides the user to move along a specific path during the experimental validation of the localization system. The measurements of the magnetic field sensors during this validation are provided to a magnetic tracking algorithm.

B. Magnetic Tracking Algorithm

Magnetic fields are generated using an in-plane array of m electromagnetic coils. A controlled magnetic force is applied on the magnetic dipole attached to a finger splint ($\mathbf{m} \in \mathbf{R}^{3\times1}$) using a controlled magnetic field $\mathbf{B}(\mathbf{p}) \in \mathbf{R}^{3\times1}$ at point $\mathbf{p}$. Let $\mathbf{p}_d \in \mathbf{R}^{3\times1}$ be the position of the magnetic dipole, and two arrays of n magnetic field sensors are fixed above and below the coils, as shown in Fig. 1(a). For the ith sensor on the upper array, the magnetic field generated by the dipole ($\mathbf{B}_{d_i}$) is given by

$$\mathbf{B}_{d_i} = \mathbf{B}_{s_i} - \sum_{j=1}^{m} \mathbf{B}_{c_{ij}} \tag{1}$$

where $\mathbf{B}_{s_i}$ and $\mathbf{B}_{c_{ij}}$ are the total magnetic field at the ith sensor and the contribution of the magnetic field generated by the jth coil, respectively. The superimposed field $\mathbf{B}_{c_{ij}}$ can be measured directly from the corresponding ith sensor at the lower array due to the magnetic symmetry of the coils. Fig. 2(a) shows a representative simulation result of the magnetic field generated by the coils. The coils are supplied with a current of 1 A. The magnetic dipole is located at the center of the coils

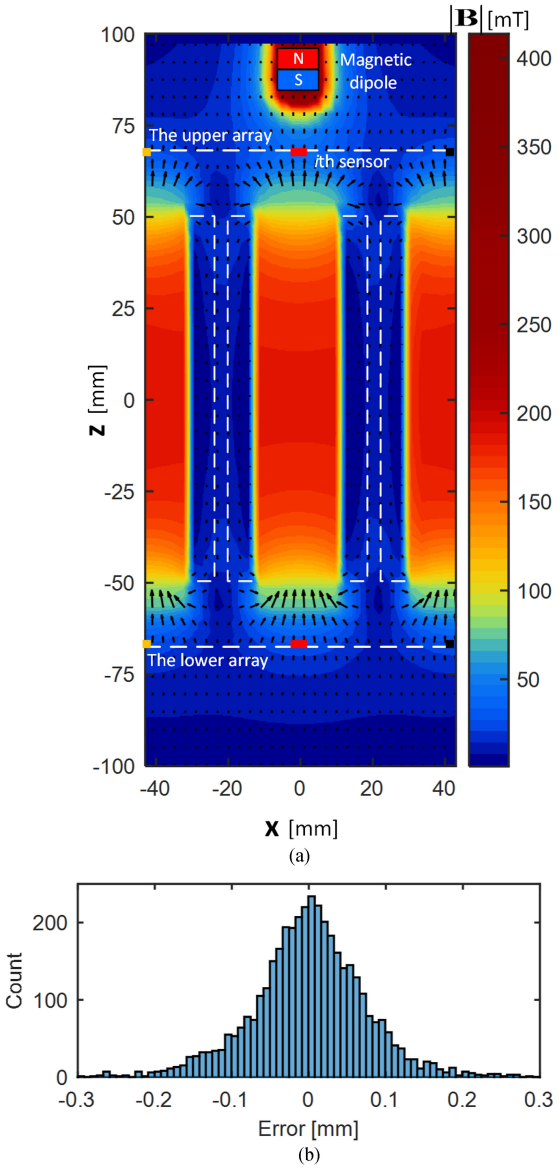

Fig. 2. Magnetic fields of the system are simulated and the neural network is trained. (a) Representative simulation result of the magnetic field generated by the electromagnetic coils for constant currents of 1 A. The magnetic dipole is located in the center of the coils at height of 30 mm from the coils. (b) Histogram of the residual mean position error for the trained neural network is calculated with a coefficient of determination of 0.999.

with height of 30 mm from the coils. The estimated position of the magnetic dipole ($\hat{\mathbf{p}}_\mathrm{d}$) is generated in three steps. The first is selection of the nearest ith sensor to the magnetic dipole $\mathbf{B}_\mathrm{d}$ by

$$\mathbf{B}_\mathrm{d} = \max_i \left|\left|\mathbf{B}_{\mathrm{d}_i}\right|\right|. \tag{2}$$

Second, the estimated position of the magnetic dipole with respect to the ith sensor ($\hat{\mathbf{p}}^i_{\mathrm{s\text{-}d}}$) is determined by a function f. This function maps the input fields ($\mathbf{B}_\mathrm{d}$) to position. A feed-forward artificial neural network is trained to approximate the function f [Cybenko 1989]. The artificial neural network estimates the position in real time without iterations [Guo 2009]. We use the MATLAB neural net fitting toolbox for building and training this network. The neural network is trained using 1300 data points around the magnetic dipole in a workspace of 50 mm × 50 mm × 50 mm. The magnetic dipole vector is perpendicular to the horizontal plane and constrained by the validation board. Measurements of the Hall effect sensors can also be used to estimate the orientation of the magnetic dipole by modifying the function f. Each data point contains the 3-D field data ($\mathbf{B}_\mathrm{m}$) corresponding to a given position $\mathbf{p}$ along the x-, y-, and z-axis. These field points are calculated by

$$\mathbf{B}_\mathrm{m} = -\mu_0 \nabla \phi(\mathbf{p}) \tag{3}$$

where μ_0 is the magnetic permeability of free space and $\phi(\mathbf{p})$ is the magnetic scalar potential. The trained neural network consists of an input, output, and ten hidden layers; each contains ten neurons. The neural network is trained using a back-propagation learning algorithm, and is implemented using the Levenberg–Marquardt technique. Fig. 2(b) shows the residual mean position error of the neural network after training, the coefficient of determination is 0.999 and the mean absolute position error (**MAE**) is 0.055 mm. Third, the position of the magnetic dipole with respect to the EHI frame of reference $\hat{\mathbf{p}}_\mathrm{d}$ is calculated using

$$\hat{\mathbf{p}}_\mathrm{d} = \mathbf{p}^i_\mathrm{s} - \hat{\mathbf{p}}^i_{\mathrm{s\text{-}d}} \tag{4}$$

where $\mathbf{p}^i_\mathrm{s}$ is a fixed vector to the ith sensor from the EHI frame of reference. The position of the magnetic dipole is used to validate the localization system under different cases of the field generated by the EHI.

III. EXPERIMENTAL VALIDATION

We conduct validation experiments under four different cases of the magnetic field generated by the EHI. These cases are likely to be encountered during haptic rendering of virtual shapes. In these experiments, the estimated position is generated by Cases 1–4 and compared to the actual position. The validation board is used to provide the actual position, as shown in Fig. 3(a). In all cases, the localization system is tested using two conditions. First, the magnetic dipole is fixed in circular holes ($n = 25$), which are distributed on the validation board. At every hole, we repeat the trails ($n = 5$) to calculate the MAE between the estimated and actual position of the hole and to investigate the repeatability of the localization system. Second, the magnetic dipole is moved along a slot located on the validation board. This slot guides the magnetic dipole to move in a predefined path. We repeat this trail ($n = 6$) for the four different cases of the field generated by the EHI. The magnetic localization system is validated in the absence of the field generated by the EHI (Case 1), and the estimated positions of the magnetic dipole in the first and second conditions are shown in Fig. 3(a). In the second and third cases, the electromagnetic coils are supplied with static (Case 2) and sinusoidal (Case 3) current inputs of 0.65 A, respectively. The electric noise in the current affects the generated magnetic fields. However, the fields of adjacent coils within the vicinity of the magnetic dipole are used to estimate its position. Therefore, the influence of the electric noise is minimized by the field subtraction. The estimated positions of the magnetic dipole in the second testing condition are shown in Fig. 3(a). The measurements of the resultant magnetic field for the ith sensor are shown in Fig. 3(b) and (c), respectively. In Case 4, the localization system is tested under time-varying magnetic fields. The coils are supplied by time-varying inputs current with a peak value of 1 A, and the estimated positions of the magnetic dipole in the second testing

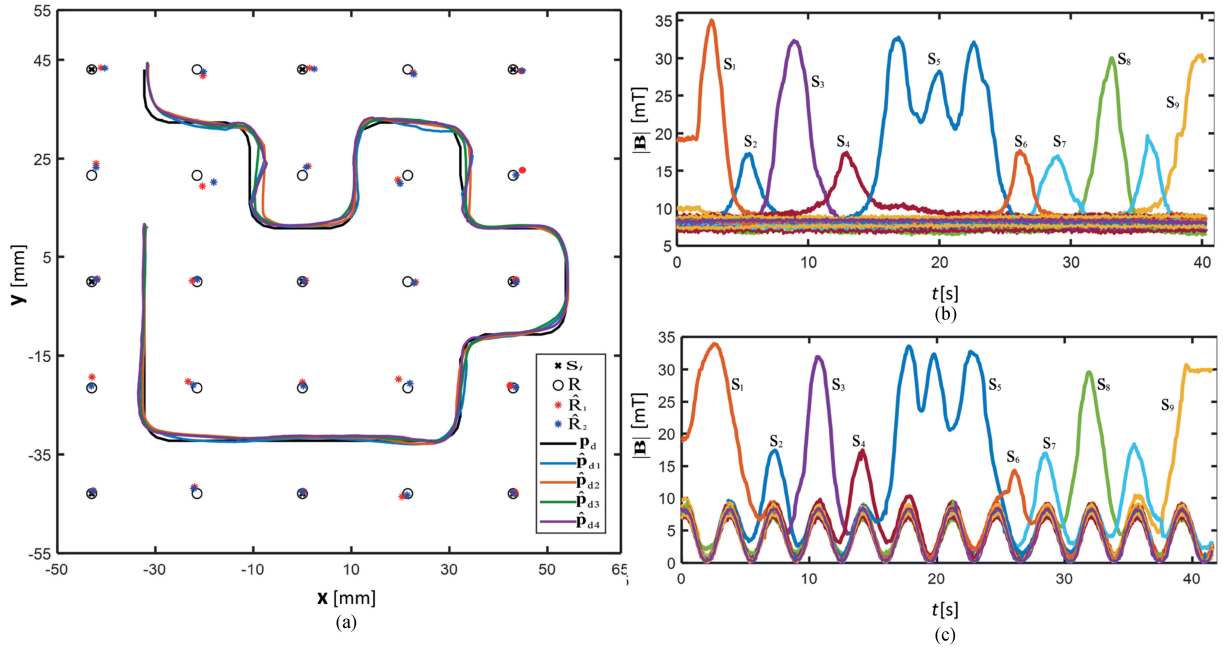

Fig. 3. Magnetic localization system is experimentally validated. (a) Results of the estimated position using S_i sensors under the absence $\hat{R}_1$ and the presence $\hat{R}_2$ of the magnetic field generated by the EHI for 25 different reference points R and a predefined path $\mathbf{p}_d$ in a two-dimensional validation board. This test is performed under four different cases of the field generated by the EHI. Zero (Case 1), static (Case 2), sinusoidal (Case 3), and time-varying magnetic field (Case 4). $\hat{\mathbf{p}}_{d1}$, $\hat{\mathbf{p}}_{d2}$, $\hat{\mathbf{p}}_{d3}$, and $\hat{\mathbf{p}}_{d4}$ are the estimated paths for Cases 1–4, respectively. (b) Resultant magnetic field generated by the magnetic dipole and the EHI during Case 2 for the ith sensor. (c) Resultant magnetic fields generated by the magnetic dipole and the EHI are measured in Case 3 for the ith sensor.

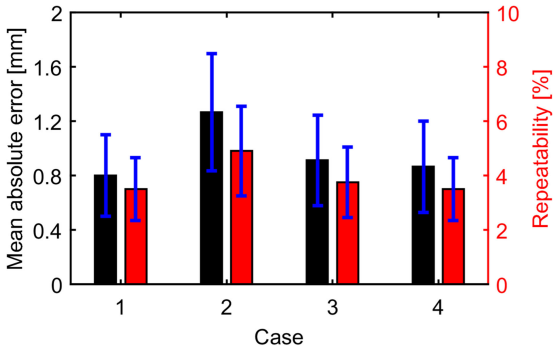

Fig. 4. Accuracy and the repeatability of the magnetic localization system are experimentally investigated. The MAEs are 0.80 ± 0.30 mm ($n = 125$), 1.26 ± 0.43 mm ($n = 125$), 0.91 ± 0.33 mm ($n = 125$), and 0.86 ± 0.33 mm ($n = 125$) for Cases 1–4, respectively. The repeatability percentages for the position data are $3.5 \pm 1.15\%$, $4.9 \pm 1.65\%$, $3.75 \pm 1.3\%$, and $3.5 \pm 1.15\%$ for Cases 1–4, respectively. Our statistical analysis shows that the repeatability of the localization system is acceptable, at $\alpha = 0.05$ and 95% confidence level.

condition are shown in Fig. 3(a). The MAEs in the first condition for Cases 2–4 are shown in Fig. 3(a).

The MAE is calculated for the four cases. Fig. 4. shows that these values are 0.80 ± 0.30 ($n = 125$), 1.26 ± 0.43 ($n = 125$), 0.91 ± 0.33 ($n = 125$), and 0.86 ± 0.33 mm ($n = 125$) for Cases 1–4, respectively. The estimated position data are examined using Gage R&R study (crossed), test-retest component to investigate the repeatability of the localization system. This test shows the percentage of variation caused by the measurement system of the total variation in the process under the same conditions. Using the analysis of variance method, this test suggests that the percentages of variation are $3.5 \pm 1.15\%$, $4.9 \pm 1.65\%$, $3.75 \pm 1.3\%$, and $3.5 \pm 1.15\%$ for Cases 1–4, respectively, as shown in Fig. 4. Our analysis shows statistical evidence to conclude that the repeatability of the proposed localization system is acceptable regardless of the field generated by the EHI, at $\alpha = 0.05$ and 95% confidence level. The total MAEs in the absence and presence of the magnetic field generated by the EHI are 0.80 ± 0.30 ($n = 125$) and 1.01 ± 0.45 mm ($n = 375$), respectively. The difference between these errors is 0.21 mm. We attribute this difference to the mechanical error in the assembly of the two arrays of magnetic field sensors and the electric noise of the coil current inputs. The localization accuracy can be improved by decreasing the mechanical assembly error and using magnetic field sensors with relatively higher sensitivity.

IV. CONCLUSION

A magnetic localization system for an EHI is developed and experimentally validated. This localization system uses the magnetic symmetry of the EHI for the elimination of its magnetic field. The proposed system is validated under four different cases of the magnetic field generated by the EHI (zero, fixed, time-varying, and random). The experimental results show that the MAE in position estimation is 1.01 ± 0.45 mm ($n = 375$). In addition, our analysis also shows statistical evidence to conclude that the repeatability of our system is acceptable regardless of the magnetic field generated by the EHI, at $\alpha = 0.05$ and 95% confidence level.

ACKNOWLEDGMENT

The authors thank Ms. D. Mahdy for her valuable feedback during preparation of this letter. This work was supported by the European Research Council under the European Union's Horizon 2020 Research and Innovation program under Grant 638428 - project ROBOTAR: Robot-Assisted Flexible Needle Steering for Targeted Delivery of Magnetic Agents.

REFERENCES

Adel A, Micheal M M, Seif M A, Abdennadher S, Khalil I S M (2018), "Rendering of virtual volumetric shapes using an electromagnetic-based haptic interface," in *Proc. IEEE Int. Conf. Intell. Robots Syst.*, Madrid, Spain, pp. 8737–8742, doi: 10.1109/IROS.2018.8593699.

Adel A, Seif M A, Hoelzl G, Kranz M, Abdennadher S, Khalil I S M (2017), "Rendering 3D virtual objects in mid-air using controlled magnetic fields," in *Proc. IEEE Int. Conf. Intell. Robots Syst.*, Vancouver, BC, Canada, pp. 349–356, doi: 10.1109/IROS.2017.8202179.

Berkelman P, Bozlee S, Miyasaka M (2013), "Interactive dynamic simulations with co-located maglev haptic and 3D graphic display," in *Proc. Int. Conf. Adv. Comput.-Human Interact.*, pp. 324–329. [Online] Available: http://www.thinkmind.org/index.php?view=article&articleid=intsys_v6_n34_2013_11

Berkelman P, Butler Z J, Hollis R L (1996), "Design of a hemispherical magnetic levitation haptic interface device," in *Proc. ASME Winter Annu. Meeting, Symp. Haptic Interfaces Virtual Environ. Teleoperator Syst.*, Atlanta, GA, USA, pp. 483–488.

Berkelman P, Hollis R L (2000), "Lorentz magnetic levitation for haptic interaction: Device design, performance, and integration with physical simulations," *Int. J. Robot. Res.*, vol. 19, pp. 644–667, doi: 10.1177/027836490001900703.

Berkelman P, Miyasaka M, Anderson J (2012), "Co-located 3D graphic and haptic display using electromagnetic levitation," in *Proc. IEEE Haptics Symp.*, Vancouver, BC, Canada, pp. 77–81, doi: 10.1109/HAPTIC.2012.6183773.

Berkelman P, Tix B, Abdul-Ghani H (2018), "Electromagnetic position sensing and force feedback for a magnetic stylus with an interactive display," *IEEE Magn. Lett.*, vol. 10, 2100505, doi: 10.1109/LMAG.2018.2886339.

Brink J B, Petruska A J, Johnson D E, Abbott J J (2014), "Factors affecting the design of untethered magnetic haptic interfaces," in *Proc. IEEE Haptics Symp.*, Houston, TX, USA, pp. 107–114, doi: 10.1109/HAPTICS.2014.6775441.

Cybenko G (1989), "Approximation by superpositions of a sigmoidal function," *Math. Control, Signals, Syst.*, vol. 2, pp. 303–314, doi: 10.1007/BF02551274.

Di Natali C, Beccani M, Valdastri P (2013), "Real-time pose detection for magnetic medical devices," *IEEE Trans. Magn.*, vol. 49, pp. 3524–3527, doi: 10.1109/TMAG.2013.2240899.

Griffiths D J (1999), *Introduction to Electrodynamics*. Englewood Cliffs, NJ, USA: Prentice-Hall.

Guo X, Yan G, He W (2009), "A novel method of three-dimensional localization based on a neural network algorithm," *J. Med. Eng. Technol.*, vol. 33, pp. 192–198, doi: 10.1080/03091900701403979.

Hashi S, Toyoda M, Yabukami S, Ishiyama K, Okazaki Y, Arai K I (2006), "Wireless magnetic motion capture system for multi-marker detection," *IEEE Trans. Magn.*, vol. 42, pp. 3279–3281, doi: 10.1109/TMAG.2006.880737.

Hu J, Chang C, Tardella N, English J, Pratt J (2005), "Effectiveness of haptic feedback in open surgery simulation and training systems," in *Medicine Meets Virtual Reality*, vol. 119. Amsterdam, The Netherlands: IOS Press, pp. 213–218.

Hu C, Li M, Song S, Yang W, Zhang R, Meng M Q-H (2010), "A cubic 3-axis magnetic sensor array for wirelessly tracking magnet position and orientation," *IEEE Sensors J.*, vol. 10, pp. 903–913, doi: 10.1109/JSEN.2009.2035711.

Hu C, Meng M Q, Mandal M (2005), "Efficient magnetic localization and orientation technique for capsule endoscopy," in *Proc. IEEE/RSJ Int. Conf. Intell. Robots Syst.*, pp. 3365–3370, doi: 10.1109/IROS.2005.1545490.

Kim D, Hilliges O, Izadi S, Butler A D, Chen J, Oikonomidis I, Olivier P (2012), "Digits: Freehand 3D interactions anywhere using a wrist-worn gloveless sensor," in *Proc. 25th Annu. ACM Symp. User Interface Softw. Technol.*, Cambridge, MA, USA, pp. 167–176, doi: 10.1145/2380116.2380139.

Ma Y, Mao Z-H, Jia W, Li C, Yang J, Sun M (2011), "Magnetic hand tracking for human–computer interface," *IEEE Trans. Magn.*, vol. 47, pp. 970–973, doi: 10.1109/TMAG.2010.2076401.

Moeslund T, Hilton A, Krüger V (2006), "A survey of advances in vision-based human motion capture and analysis," *Comput. Vis. Image Understanding*, vol. 104, pp. 90–126, doi: 10.1016/j.cviu.2006.08.002.

Petruska A J, Abbott J J (2013), "Optimal permanent-magnet geometries for dipole field approximation," *IEEE Trans. Magn.*, vol. 49, pp. 811–819, doi: 10.1109/TMAG.2012.2205014.

Popek K M, Hermans T, Abbott J J (2017), "First demonstration of simultaneous localization and propulsion of a magnetic capsule in a lumen using a single rotating magnet," in *Proc. IEEE Int. Conf. Robot. Autom.*, Singapore, pp. 1154–1160, doi: 10.1109/ICRA.2017.7989138.

Salcudean S E, Vlaar T D (1997), "On the emulation of stiff walls and static friction with a magnetically levitated input/output device," *J. Dyn. Syst., Meas. Control*, vol. 119, pp. 127–132, doi: 10.1115/1.2801204.

Schlageter V, Besse P-A, Popovic R S, Kucera P (2001), "Tracking system with five degrees of freedom using a 2D-array of Hall sensors and a permanent magnet," *Sensors Actuators A, Phys.*, vol. 92, pp. 37–42, doi: 10.1016/S0924-4247(01)00537-4.

Seif M A, Hassan A, El-Shaer A H, Alfar A, Misra S, Khalil I S M (2017), "A magnetic bilateral tele-manipulation system using paramagnetic microparticles for micromanipulation of nonmagnetic objects," in *Proc. IEEE Int. Conf. Adv. Intell. Mechatronics*, Munich, Germany, pp. 1095–1102, doi: 10.1109/AIM.2017.8014165.

Son D, Yim S, Sitti M (2016), "A 5-D localization method for a magnetically manipulated untethered robot using a 2-D array of Hall-effect sensors," *IEEE/ASME Trans. Mechatronics*, vol. 21, pp. 708–716, doi: 10.1109/TMECH.2015.2488361.

Tong Q, Yuan Z, Liao X, Zheng M, Yuan T, Zhao J (2018), "Magnetic levitation haptic augmentation for virtual tissue stiffness perception," *IEEE Trans. Vis. Comput. Graph.*, vol. 24, pp. 3123–3136, doi: 10.1109/TVCG.2017.2772236.

Weitschies W, Wedemeyer J, Stehr R, Trahms L (1994), "Magnetic markers as a non-invasive tool to monitor gastrointestinal transit," *IEEE Trans. Biomed. Eng.*, vol. 41, pp. 192–195, doi: 10.1109/10.284931.

Yim S, Sitti M (2013), "3-D Localization method for a magnetically actuated soft capsule endoscope and its applications," *IEEE Trans. Robot.*, vol. 29, pp. 1139–1151, doi: 10.1109/TRO.2013.2266754.

Zhang Q, Dong H, El Saddik A (2016), "Magnetic field control for haptic display: System design and simulation," *IEEE Access*, vol. 4, pp. 299–311, doi: 10.1109/ACCESS.2016.2514978.